A Robust Collision Perception Visual Neural Network With Specific Selectivity to Darker Objects

Qinbing Fu, *Member, IEEE*, Cheng Hu, Jigen Peng, F. Claire Rind, and Shigang Yue, *Senior Member, IEEE*

***Abstract*—Building an efficient and reliable collision perception visual system is a challenging problem for future robots and autonomous vehicles. The biological visual neural networks, which have evolved over millions of years in nature and are working perfectly in the real world, could be ideal models for designing artificial vision systems. In the locust's visual pathways, a lobula giant movement detector (LGMD), that is, the LGMD2, has been identified as a looming perception neuron that responds most strongly to darker approaching objects relative to their backgrounds; similar situations which many ground vehicles and robots are often faced with. However, little has been done on modeling the LGMD2 and investigating its potential in robotics and vehicles. In this article, we build an LGMD2 visual neural network which possesses the similar collision selectivity of an LGMD2 neuron in locust via the modeling of biased-ON and -OFF pathways splitting visual signals into parallel ON/OFF channels. With stronger inhibition (bias) in the ON pathway, this model responds selectively to darker looming objects. The proposed model has been tested systematically with a range of stimuli including real-world scenarios. It has also been implemented in a micro-mobile robot and tested with real-time experiments. The experimental results have verified the effectiveness and robustness of the proposed model for detecting darker looming objects against various dynamic and cluttered backgrounds.**

***Index Terms*—Collision perception, darker objects selectivity, lobula giant movement detectors (LGMD)2, ON and OFF pathways, mobile robots, neuron model.**

Manuscript received February 25, 2019; revised July 2, 2019 and September 20, 2019; accepted September 29, 2019. This work was supported in part by EU Horizon 2020 through Project STEP2DYNA under Grant 691154 and Project ULTRACEPT under Grant 778062, and in part by the National Natural Science Foundation of China under Grant 11771347. This article was recommended by Associate Editor Q. Meng. *(Qinbing Fu is first author.) (Corresponding author: Shigang Yue.)*

Q. Fu, C. Hu, and S. Yue are with the Machine Life and Intelligence Research Centre, School of Mechanical and Electrical Engineering, Guangzhou University, Guangzhou 510006, China, and also with the Computational Intelligence Lab/Lincoln Centre for Autonomous Systems, School of Computer Science, University of Lincoln, Lincoln LN6 7TS, U.K. (e-mail: qifu@lincoln.ac.uk; syue@lincoln.ac.uk).

J. Peng is with the School of Mathematics and Information Science, Guangzhou University, Guangzhou 510006, China.

F. C. Rind is with the Institute of Neuroscience, Newcastle University, Newcastle NE1 7RU, U.K., and also with the Centre for Behaviour and Evolution, Newcastle University, Newcastle NE1 7RU, U.K.

This article has supplementary downloadable material available at http://ieeexplore.ieee.org, provided by the author.

Color versions of one or more of the figures in this article are available online at http://ieeexplore.ieee.org.

Digital Object Identifier 10.1109/TCYB.2019.2946090

I. Introduction

COLLISIONS happen at every second in the real world, which often result in serious accidents and fatalities. In the future, every kind of artificial mobile machines, such as ground vehicles, robots, and unmanned aerial vehicles (UAVs), should have good capability to detect and avoid collisions. However, current approaches for collision detection, such as radar, laser, infrared, ultrasound, vision sensors, or combinations of these are far from an acceptable level in terms of reliability, energy consumption, price, and size. A new type of reliable, low cost, energy efficient, and miniaturized collision detection sensors is required to make future autonomous mobile machines safe to serve human society.

In nature, insects, though with tiny brains, possess almost perfect sensory systems for timely collision sensing and avoidance within dynamic environments. As examples of visually guided navigation, it was discovered early on that locusts can see in light levels equivalent to starlight during migratory flights [1], and fly in swarms for hundreds of miles free of collision [2]. Nocturnal insects successfully forage in the forest at night without collision [3], [4]. The underlying mechanisms in biological visual pathways are prominent and powerful model systems to build collision-detecting systems, as reviewed in [5]–[8].

Specifically, a group of lobula giant movement detectors (LGMDs) in the locust's visual system has been discovered sensitive to looming objects [9]–[15]. The LGMD1 was first identified as a movement detector and gradually recognized as a looming objects detector, e.g., [11] and [15]. In the same lobula layer, the LGMD2 was identified as a darker looming objects detector with unique characters that are different to the LGMD1, that is, the LGMD2 lacks a ventrally located feedforward inhibitory (FFI) pathway which conveys object-size-dependent inhibition to directly suppress the neuron [12], as illustrated in Fig. 1. Though both giant neurons are physically close to each other and have similar presynaptic structures, the LGMD2 possesses different selectivity to only darker objects moving in depth relative to their backgrounds [12], [14].

Computationally, modeling such fascinating looming sensitive neurons will not only deepen our understanding of the very complex biological visual processing but also shed light on building robust collision perception visual systems for robots and vehicles. In the past decade, the LGMD1 neuron has been

modeled with a good number of studies and tested in ground robots, e.g., [16]–[19], and recently in UAVs [20], [21]. These LGMD1-based modeling studies have demonstrated that the biological visual systems can be good paradigms to develop energy efficient and reliable collision detection visual systems for real-world applications.

Compared with the LGMD1, the LGMD2 neuron only detects darker objects that approach within a bright background rather than any other categories of visual movements. Realizing this feature will undoubtedly enhance the selectivity to collisions caused by darker approaching objects. However, very little LGMD2 modeling work has been done to demonstrate its collision-detecting ability and potential in real-world applications, due to two main aspects of difficulties.

1) On the aspect of biology, the LGMD2's neural circuitry still remains largely unknown compared with the LGMD1, including both its presynaptic structure and postsynaptic target neuron [15]. Therefore, understanding the LGMD2's underlying neural mechanisms forming its specific selectivity to only darker looming objects is difficult.
2) Regarding computational modeling, implementing the LGMD2's specific collision selectivity to only darker objects has always been a challenging problem. Until recent years, the research progress made by biologists on biological ON and OFF pathways for motion perception [22], [23] has promoted the proposed LGMD2 modeling study with speculations that such dual-pathways exist also in the LGMD2's presynaptic circuit (see subfield A in Fig. 1) to fulfill its specific characteristics.

Building upon our early partial studies on the LGMD2 [24]–[26], this article investigates the LGMD2's unique features through systematic modeling and experimental research and demonstrates its potential as a robust collision perception visual system for mobile robots. The main contributions of this article can be summarized as follows.

1) This article proposes the first systematic modeling study of the LGMD2 in the locust's visual system. For the first time, the LGMD2's specific characteristics and selectivity to only darker objects has been realized by the proposed visual neural network.
2) The proposed modeling of ON and OFF pathways can implement both the LGMD1 [17] and the proposed LGMD2 which evidences that such structures and mechanisms play roles in the locust's visual system, though little physiological and anatomical evidence has been found to date.
3) We develop a novel adaptive inhibition mechanism that works effectively to adjust local lateral inhibitions for shaping the LGMD2's unique selectivity at some critical moments by rapid or large-field movements. The model produces a similar response to the locust LGMD2 [12].
4) This article yields a simple and effective vision-based collision detection solution for mobile machines like robots that requires only an ordinary camera system and few computational resources.

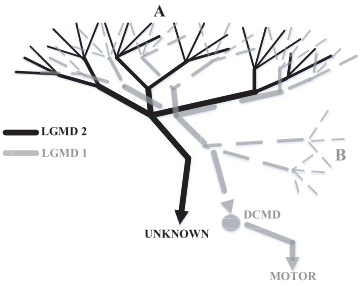

Fig. 1. Schematic of the LGMDs morphology. Subfield A indicates the presynaptic dendritic structures of both LGMDs. Subfield B indicates the FFI pathway of LGMD1 which is absent from LGMD2 [12]. DCMD is a one-to-one postsynaptic target neuron to LGMD1 conveying neural signals to motor; the partner neuron of LGMD2 remains unknown [12], [15].

The remainder of this article is organized as follows. Section II reviews the relevant fields of studies. Section III introduces the proposed LGMD2 visual neural network. Section IV presents the systematic experiments and results. Further discussion is given in Section V. Section VI concludes this article.

II. Related Work

Within this section, we briefly review related works in the areas of: 1) conventional computer vision techniques for collision detection; 2) bioinspired methods for collision detection; 3) neural properties of the LGMD2, notably the differences to the LGMD1; and 4) ON and OFF pathways in both biological and artificial vision systems.

A. Computer Vision for Collision Detection

For real-time collision detection, the vast majority of computer vision methods apply object-scene segmentation, estimation, localization, or classification-based algorithms [27], [28]. Some collision detectors have been used in ground vehicles [27] and UAVs [29] for the purpose of improving navigation safety. As emergence of new types of visual sensors like RGB-D, e.g., [30] and [31] and event-driven cameras, e.g., [32] and [33], the collision detection strategies can be enriched with more abundant visual features extracted for implementing obstacle recognition, object segmentation, map construction, etc. More specifically, compared with standard cameras, these new visual sensors have a very high dynamic range that guarantees good performance to detect high-speed motions [33].

However, the conventional computer vision techniques for collision detection are either computationally costly or heavily reliant on specialized visual sensors. In addition, the efficiency and performance of these approaches also depend on the complexity of real physical scenes. Therefore, a new type of miniaturized, low cost, low power, and reliable visual collision detectors is demanded for future intelligent machines interacting within complex dynamic environments.

B. Biologically Inspired Visual Collision Detectors

Millions of years of evolutionary development has endowed, in nature, animals with robust and efficient collision-detecting

visual systems. As outstanding examples, flying insects that demonstrate amazing collision perception and avoidance abilities, have been researched with considerable biological and modeling studies [5]–[8]. More concretely, a significant number of models come from optic flow (OF)-based strategies in the flying insects' visual systems [8]. The OF-based method has been successfully applied to a variety of flying robots for guiding insect-like behaviors including collision avoidance in flight [5], [7], [34], [35]. Such a strategy mimics the functionality of bilateral compound eyes of flying insects at the ommatidia level. The local apparent motion flows containing direction and intensity information are captured and computed by "delay-and-correlation" algorithms [5], [8], [22]. A field of local motion vectors is thus formed. However, to the best of our knowledge, a limitation exists that it is mainly used for sensing lateral rather than frontal collision threats.

On the other hand, the giant neurons like the LGMD1 in the locust's visual systems respond most strongly to frontal looming objects over other kinds of movements [11], [15], [36], [37]. As a powerful model system, the LGMD1 has been built as a quick collision detector and applied to ground vehicle scenarios, e.g., [38]–[40]; mobile robots, e.g., [16]–[18] and [41]; and UAVs [20], [21], and also embodied in hardware implementation like the field programmable gate array (FPGA) [42]. Compared with the OF-based approaches, the LGMD1 models detect potential collisions by reacting to expanding edges of objects that approach. With similar ideas, Yue and Rind [43] computationally modeled another group of directionally selective neurons (DSNs) in locusts for collision detection. Compared with the LGMD1-based models, the DSNs visual neural networks can provide additional edge-direction information of looming objects.

In general, most of these bioinspired systems have been used to guide mobile robots in navigation. They nevertheless work individually; integrating different methods in the future could further enhance robots' obstacle avoidance capabilities.

C. Characterization of the LGMD2

In comparison with the LGMD1, few biological [12], [14], [15] and modeling [24]–[26] studies have touched upon the LGMD2 due to the difficulties mentioned in the last section. Similar to the LGMD1, the LGMD2 responds selectively to looming objects, with increasing firing rates peaked before the objects reaching a particular angular size in the field of view [12]. It is rigorously inhibited during either the whole-field luminance change or grating movements [12]. Moreover, when challenged by translation with constant intensity, the LGMD2 is excited for a short while then inhibited very soon, early before the end of translation [12] (see Fig. 4).

Not limited to that, biologists have recognized the LGMD2's unique looming selectivity. A notable feature of the LGMD2 is that it is only sensitive to darker approaching objects against a bright background, while not able to detect brighter or white objects approaching within dark background [12]. Furthermore, biologists have also realized that the LGMD2 has a preference for the light-to-dark luminance transitions (or OFF contrast). For example, only the direction of movement of a single dark edge advancing rightward or a single light edge retracting with OFF contrast excites the LGMD2 [12] (see Fig. 4 in Section IV). In contrary, the LGMD1 responds to both the dark-to-light luminance change (or ON contrast) and OFF contrast [17]. The LGMD2's characteristics make it outside of normal expectation and a unique neuron to model.

D. ON *and* OFF *Pathways for Motion Perception*

The proposed LGMD2 visual neural network is featured by a new bio-plausible structure of the ON and OFF pathways which separates the visual processing from the photoreceptor layer into parallel computation. The ON and OFF pathways have been discovered in the preliminary visual systems of many animal species, such as insects like flies [22], [44], and vertebrates [45] including rabbits [22], mice [23], cats [46], and monkeys [47]. Such a structure reveals an essential principle of biological visual processing, that is, the motion information is separated into parallel ON and OFF channels encoding brightness increments (ON) and decrements (OFF), separately [22], [23], [48]. For locusts, there is very limited evidence showing or suggesting the existence of such polarity mechanisms [10], [13], [15], [49].

With regard to locust LGMDs-based modeling studies, a seminal LGMD1 work applied similar ON and OFF mechanisms for collision detection in real-world scenarios [50]. Recent researches also demonstrated the effectiveness of such a novel structure to implement a biological LGMD1 [17], [40].

III. Formulation of the Visual Neural Network

Within this section, the proposed method will be presented in detail. We first introduce the core structures of the LGMD2 visual neural network, then elaborate on its components in the following sections.

To achieve the LGMD2's specific selectivity to darker objects, we highlight the modeling of biased-ON and OFF pathways and adaptive inhibition mechanism. Generally speaking, the proposed visual neural network consists of five layers, including photoreceptor (P), excitation (E), inhibition (I), summation (S), and grouping (G) layers and an LGMD2 cell. The E, I, and S layers are embodied in the parallel ON and OFF pathways. As illustrated in Fig. 2, the luminance change at local pixel level is captured by the P layer; the luminance increments flow into ON channels; whilst the decrements flow into OFF channels; each polarity pathway depicts spatiotemporal neural computation between local excitations and inhibitions; notably, the stronger inhibition (namely, "bias") is put forth in the ON pathway to achieve the LGMD2's unique selectivity to darker objects moving in depth; all the presynaptic local excitations reaching the LGMD2 are integrated to form the membrane potential which is then shaped by a spike frequency adaptation (SFA) mechanism and generating spikes to indicate potential collision threats by darker objects. Moreover, the adaptive inhibition mechanism is accomplished by a photoreceptors mediation (PM) pathway to adjust local biases on lateral inhibitions in either ON/OFF pathway.

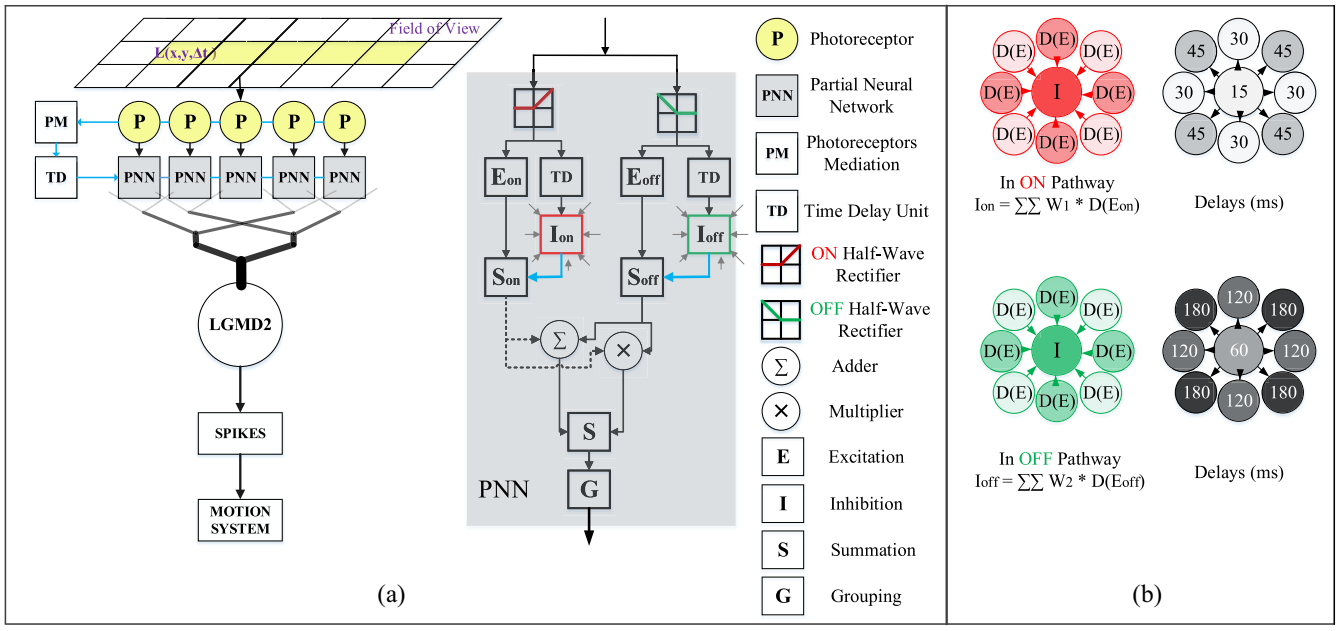

Fig. 2. Schematic of the (a) LGMD2 visual neural network and (b) spatiotemporal convolution. For clear illustration, only five photoreceptors and corresponding downstream processing are depicted. Each photoreceptor captures luminance (L) change at local pixel level within the field of view. Each connects with a partial neural network, that is, ON and OFF channels. The LGMD2 cell integrates the entire presynaptic local excitations. A separate PM pathway (blue lines) adjusts the local inhibitory strength in either ON/OFF channel, at every time step. The local ON/OFF inhibitions are generated by convolving surrounding delayed ON/OFF excitations. Stronger inhibitions are formed in all the ON channels to sieve the ON excitations (dashed lines).

Our motivation to introduce the two core structures in this modeling research is mainly based on the following points.

1) The ON and OFF pathways work effectively to separate different collision selectivity between the LGMD1 and the LGMD2, and can implement functions of both the LGMDs. With speculations that the ON channels are rigorously sieved by stronger lateral inhibitions, the specific selectivity of LGMD2 can be separated from the LGMD1. As a result, such a structure could be used to construct a general model for the locust's looming sensitive giant neurons.
2) The biological LGMD2 lacks the FFI pathway in the LGMD1's circuitry (see subfield B in Fig. 1), but represents similar inhibitions to the LGMD1 on rapid or large-field luminance change. To achieve this, the proposed LGMD2 model is characterized by a new adaptive inhibition mechanism to adjust local lateral inhibitions in both polarity pathways adapting to various visual movements.

A. Photoreceptors Layer

The first computational layer consists of photoreceptors arranged in a matrix, which captures the grayscale luminance and computes the temporal derivative of every pixel to get motion information [11], [17], [51]. Let $L(x, y, t) \in \mathbb{R}^3$ denotes the input image streams, where x, y, and t are spatial and temporal positions, respectively. The computation can be defined as

$$P(x, y, t) = L(x, y, t) - L(x, y, t-1) + \sum_{i=1}^{n_p} a_i \cdot P(x, y, t-i) \tag{1}$$

$$a_i = \left(1 + e^i\right)^{-1} \tag{2}$$

where $P(x, y, t)$ denotes the luminance change of pixel (x, y) with respect to time t. The persistence of luminance change could last for a short while of n_p number of frames [51], and a_i stands for a decay coefficient.

B. ON and OFF Mechanisms

After that, motion information is passed into separated ON/OFF channels, that is, the start of visual processing in the ON and OFF pathways. The functions of ON and OFF transient cells are implemented by half-wave rectifying. More precisely, for each photoreceptor, the luminance increment flows into the ON channel, whilst the brightness decrement flows into the OFF channel, that is

$$\begin{aligned} P_{\text{on}}(x, y, t) &= \left[P(x, y, t)\right]^+ + \alpha_1 \cdot P_{\text{on}}(x, y, t-1) \\ P_{\text{off}}(x, y, t) &= -\left[P(x, y, t)\right]^- + \alpha_1 \cdot P_{\text{off}}(x, y, t-1). \end{aligned} \tag{3}$$

Here, $[x]^+$ and $[x]^-$ denote $\max(0, x)$ and $\min(x, 0)$, respectively. A small fraction (α_1) of residual signals is allowed to pass through. Such mechanisms have also demonstrated the efficacy to encode other insect-inspired motion detectors, including small target movement detectors of the flying insects [52], [53] and angular velocity detectors of the bee [54], [55] and direction-selective neurons of the *Drosophila* [56], [57].

C. Neural Computation in ON and OFF Pathways

In the previous LGMD1-based models, e.g., [11], [17], [41], and [51], there are two kinds of signal flows, that is, the excitation and the inhibition competing with each other. If the

former one wins, the neuron is activated to spike; otherwise, the neuron remains quiet. More precisely, the lateral inhibitions are time delayed which cut down the motion-dependent excitations with an object growing on the visual field. Such a competition plays crucial roles of shaping the looming selectivity of the locust's giant neurons. For modeling the LGMD2, we apply similar strategies: each pathway depicts the competition between local polarity excitations and inhibitions. For implementing the LGMD2's specific selectivity, the stronger inhibitions are put forth in all the ON channels forming a biased-ON pathway.

1) Competition in the ON *Pathway:* In the ON pathway, the local excitation (E) reaches the E_{on} unit without temporal latency; meanwhile, it is fed into a time-delay unit (TD). The local inhibition (I) in the I_{on} unit is thus formed by convolving surrounding delayed local excitations $\hat{E}_{\text{on}}$ [see $D(E_{\text{on}})$ in Fig. 2(b)]. The entire process can be defined as

$$E_{\text{on}}(x, y, t) = P_{\text{on}}(x, y, t) \tag{4}$$

$$\hat{E}_{\text{on}}(x, y, t) = \alpha_2 E_{\text{on}}(x, y, t) + (1 - \alpha_2) E_{\text{on}}(x, y, t - 1) \tag{5}$$

$$\alpha_2 = \tau_{\text{in}}/(\tau_1 + \tau_{\text{in}}) \tag{6}$$

$$I_{\text{on}}(x, y, t) = \sum_{i=-1}^{1} \sum_{j=-1}^{1} \hat{E}_{\text{on}}(x + i, y + j, t) W_1(i + 1, j + 1). \tag{7}$$

τ_1 and τ_{in} are two time constants in milliseconds, wherein τ_1 stands for the excitation delay time [see Fig. 2(b)], and τ_{in} is the time interval between the consecutive frames of digital signals. W_1 stands for a convolution kernel that meets the following matrix:

$$W_1 = \begin{pmatrix} 1/4 & 1/2 & 1/4 \\ 1/2 & 2 & 1/2 \\ 1/4 & 1/2 & 1/4 \end{pmatrix}. \tag{8}$$

In the convolution process, the center cell has the highest weighting and the shortest delay; the four nearest cells have the moderate weighting and delay; and the four diagonal cells share the lowest weighting and longest delay [see Fig. 2(b)]. The selection of spatiotemporal parameters originates from the biological research on the LGMD [15]: the delayed signal flows spread out to their surrounding area to form lateral inhibitions affecting and cutting down the motion-dependent excitations.

2) Competition in the OFF *Pathway:* In the OFF pathway, signal flows conveyed by the OFF cells form the local excitations to the E_{off} unit without latency, and the delayed local inhibitions $\hat{E}_{\text{off}}$ [see $D(E_{\text{off}})$ in Fig. 2(b)] in the I_{off} unit. These processes are defined as

$$E_{\text{off}}(x, y, t) = P_{\text{off}}(x, y, t) \tag{9}$$

$$\hat{E}_{\text{off}}(x, y, t) = \alpha_3 E_{\text{off}}(x, y, t) + (1 - \alpha_3) E_{\text{off}}(x, y, t - 1) \tag{10}$$

$$\alpha_3 = \tau_{\text{in}}/(\tau_2 + \tau_{\text{in}}) \tag{11}$$

$$I_{\text{off}}(x, y, t) = \sum_{i=-1}^{1} \sum_{j=-1}^{1} \hat{E}_{\text{off}}(x + i, y + j, t) W_2(i + 1, j + 1). \tag{12}$$

Compared with the ON channels, the delay time constant τ_2 at each local cell is larger [see Fig. 2(b)]: prolonging the delay will reduce the local inhibitions. W_2 fits the following matrix with lower weightings:

$$W_2 = \begin{pmatrix} 1/8 & 1/4 & 1/8 \\ 1/4 & 1 & 1/4 \\ 1/8 & 1/4 & 1/8 \end{pmatrix}. \tag{13}$$

Following the generation of local ON/OFF excitations and inhibitions, there are local ON/OFF summation (S) cells in both channels depicting a purely linear computation, that is

$$\begin{aligned} S_{\text{on}}(x, y, t) &= \left[E_{\text{on}}(x, y, t) - w_1(t) \cdot I_{\text{on}}(x, y, t)\right]^+ \\ S_{\text{off}}(x, y, t) &= \left[E_{\text{off}}(x, y, t) - w_2(t) \cdot I_{\text{off}}(x, y, t)\right]^+ \end{aligned} \tag{14}$$

where $w_1(t)$ and $w_2(t)$ are time-varying local biases to control the intensity of inhibitory flows.

D. Adaptive Inhibition Mechanism

As introduced in Sections I and II, the LGMD2 circuitry lacks the FFI pathway which can directly suppress the neuron if luminance changes rapidly over a large area in the field of view. However, the LGMD2 also shows a similar vigorous inhibition in the physiological experiments [12], at some critical moments of either the end of approach by darker objects or the start of recession by brighter objects. To fulfill this character, we propose the original modeling of adaptive inhibition mechanism to adjust the ON and OFF time-varying biases in (14). As illustrated in Fig. 2, this is implemented by a PM pathway with a slight delay, which is given by

$$\text{PM}(t) = \sum_{x=1}^{R} \sum_{y=1}^{C} |P(x, y, t)| \cdot (C \cdot R)^{-1} \tag{15}$$

$$\hat{\text{PM}}(t) = \alpha_4 \text{PM}(t) + (1 - \alpha_4) \text{PM}(t - 1), \;\; \alpha_4 = \tau_{\text{in}}/(\tau_3 + \tau_{\text{in}}) \tag{16}$$

$$w_1(t) = \max\left(w_3, \frac{\hat{\text{PM}}(t)}{T_{pm}}\right), \;\; w_2(t) = \max\left(w_4, \frac{\hat{\text{PM}}(t)}{T_{pm}}\right). \tag{17}$$

C and R denote the columns and rows of the photoreceptors layer; and τ_3 stands for a delay time constant. T_{pm} is a predefined threshold; and w_3 and w_4 denote the different baselines of bias in ON and OFF pathways, respectively. In addition, this novel mechanism works effectively to enable the LGMD2 model to adapt to different levels of background complexity. More precisely, the local lateral inhibition gets stronger when luminance changes dramatically within the field of view. This mechanism well accounts for the explored physiological features of the LGMD2 [12], with which the giant neuron is inhibited by large-field movements, such as gratings, rapid turning scenes, end of approach, start of recession, etc. Performing in the real physical world, this can also enhance the LGMD2's selectivity to darker objects that approach over other categories of movements against various dynamic backgrounds.

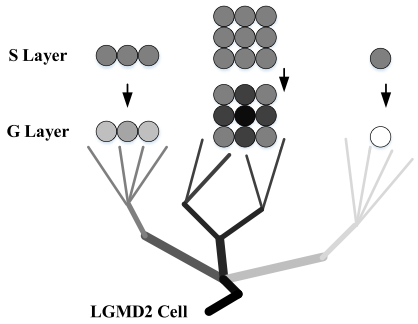

Fig. 3. Schematic illustration of G layer processing. The S cells surrounded by strong excitations gain bigger passing coefficients; the isolated ones get smaller passing coefficients and may be ruled out in the G layer by threshold. Circles represent the excitations in the S and G layers. The excitation strength is indicated by gray levels, where black represents the strongest excitation.

E. Summation and Grouping Layers

As exhibited in the partial neural network (PNN) of Fig. 2, there are interactions between local excitations from the ON and OFF channels in the summation (S) unit. The calculation obeys a supralinear rule as

$$S(x,y,t) = \theta_1 \cdot S_{\text{on}}(x,y,t) + \theta_2 \cdot S_{\text{off}}(x,y,t) + \theta_3 \cdot S_{\text{on}}(x,y,t) \cdot S_{\text{off}}(x,y,t) \quad (18)$$

where $\{\theta_1, \theta_2, \theta_3\}$ denote the combination of term coefficients that allows the S unit to represent different "balances" between local polarity excitations and mediate influences by ON and OFF contrast. This method can realize either linear or multiplicative neural computation, which has demonstrated the effectiveness of implementing the small target movement detector [48] and also the LGMD1 [17]. For the proposed model, this can also play a role of enhancing the LGMD2's preference for OFF contrast.

Cascaded the S layer, the proposed neural network is featured by a grouping (G) layer (see Fig. 3), for the purpose of reducing isolated noise and improving the extraction of colliding objects against complex backgrounds with detail noise [51]. This is implemented with a passing coefficient matrix Ce obtained by a convolution process with an equal-weighted kernel W_g, that is

$$Ce(x,y,t) = \sum_{i=-1}^{1}\sum_{j=-1}^{1} S(x+i, y+j, t) W_g(i+1, j+1) \quad (19)$$

$$W_g = \frac{1}{9} \times \begin{pmatrix} 1 & 1 & 1 \\ 1 & 1 & 1 \\ 1 & 1 & 1 \end{pmatrix} \quad (20)$$

$$G(x,y,t) = S(x,y,t) \cdot Ce(x,y,t) \cdot \omega(t)^{-1} \quad (21)$$

$$\omega(t) = \max([Ce]_t) \cdot C_\omega^{-1} + \Delta_C. \quad (22)$$

ω is a scale parameter computed at every time step; C_ω is a constant; and Δ_C stands for a small real number. Furthermore, the isolated and decayed excitations are filtered by

$$\hat{G}(x,y,t) = \begin{cases} G(x,y,t), & \text{if } G(x,y,t) \cdot C_{\text{de}} \geq T_{\text{de}} \\ 0, & \text{otherwise} \end{cases} \quad (23)$$

where C_{de} stands for the decay coefficient and $C_{\text{de}} \in (0, 1)$; and T_{de} denotes the decay threshold. As a result, the grouped excitations in the S layer representing expanding edges become stronger when reaching the G layer and the background details caused isolated excitations are largely filtered out.

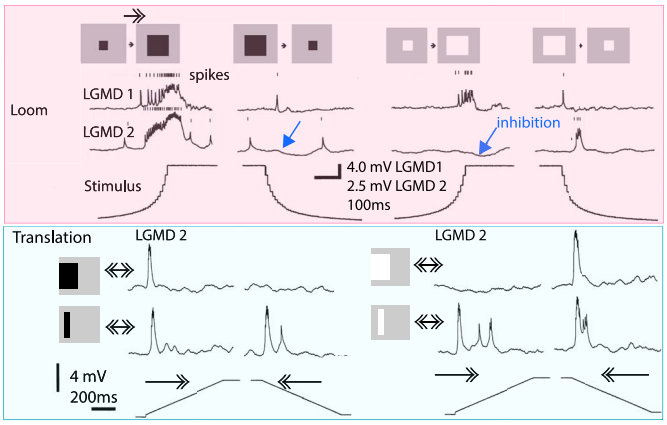

Fig. 4. Biological data on the LGMD2 neural responses to darker and lighter objects looming and translating, adapted from [12]. The LGMD1 responds to all stimuli of looming, translating, and elongating-shortening (a single-edge translating); whilst the LGMD2 responds selectivity to darker object approaching, briefly to translation, lighter object receding, darker object elongating, and lighter object shortening—the preference for OFF contrast.

F. LGMD2 Cell

After the presynaptic visual processing, an LGMD2 cell integrates all local excitations from the G layer to form the membrane potential as the following:

$$k(t) = \sum_{x=1}^{R}\sum_{y=1}^{C} \hat{G}(x,y,t), \quad K(t) = \left(1 + e^{-k(t)\cdot(C\cdot R\cdot\alpha_5)^{-1}}\right)^{-1} \quad (24)$$

where α_5 denotes a scale coefficient, and the output is regulated within [0.5, 1).

Subsequently, following our recent modeling studies on biological LGMDs [17], [25], [40], we apply an SFA mechanism to further sharpen up the LGMD2's selectivity, which is defined as

$$\hat{K}(t) = \begin{cases} \alpha_6\left(\hat{K}(t-1) + K(t) - K(t-1)\right) \\ \text{if } (K(t) - K(t-1)) \leq T_{sfa} \\ \alpha_6 K(t), \quad \text{otherwise} \end{cases} \quad (25)$$

$$\alpha_6 = \tau_4/(\tau_4 + \tau_{\text{in}}) \quad (26)$$

where α_6 is a coefficient that indicates adaptation rate to visual movements; T_{sfa} denotes a small real number as the threshold; and τ_4 is a delay time constant. Generally speaking, such a mechanism is a reduction of neuron firing rate to stimuli with constant or decreasing intensity, e.g., objects recede or translate at a constant speed; it has little effect on accelerating motion with increasing intensity like looming [17]. The SFA mechanism is sensitive to the motion intensity gradient and ideal for shaping the LGMD2's response to darker objects approaching rather than merely translating or brighter objects receding, which can be clearly seen from the testing results in Figs. 5–7 in Section IV.

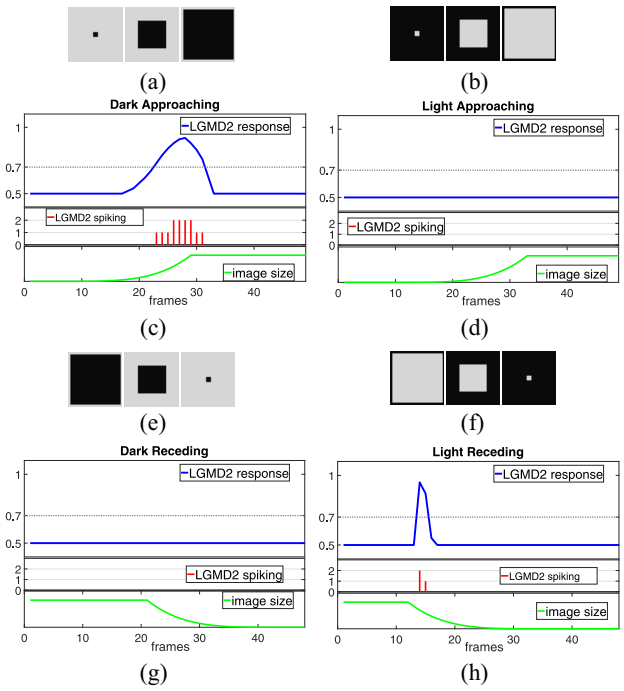

Fig. 5. Proposed LGMD2 model outputs by darker and brighter objects approaching and receding: membrane potential and spikes are depicted with the change of image size shown at each bottom, the horizontal dashed line indicates firing threshold at 0.7. The output at 0.5 indicates nonresponse. (a) Dark looming. (b) Bright looming. (c), (d), (g), and (h) Model outputs. (e) Dark recession. (f) Bright recession.

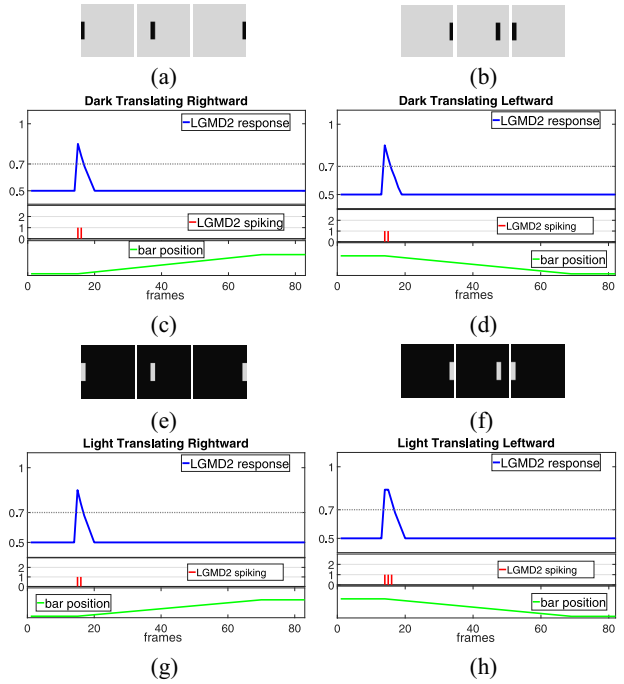

Fig. 6. LGMD2 outputs by darker and brighter bars translating rightward (R) and leftward (L) with the change of bar position depicted at each bottom. (a) Dark translation-R. (b) Dark translation-L. (c), (d), (g), and (h) Model outputs. (e) Bright translation-R. (f) Bright translation-L.

After that, the membrane potential is exponentially mapped to spikes by an integer-valued function, that is

$$S^{\text{spike}}(t) = \left[e^{\left(\alpha_7 \cdot \left(\hat{K}(t) - T_{spi}\right)\right)} \right] \tag{27}$$

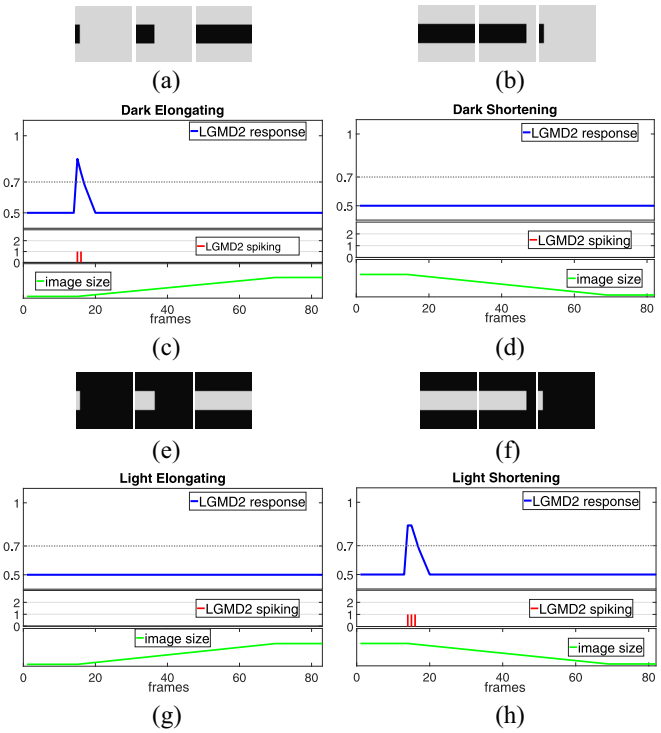

Fig. 7. LGMD2 outputs by dark and light elongation and shortening movements with the change of image size depicted at each bottom. (a) Dark elongation. (b) Dark shortening. (c), (d), (g), and (h) Model outputs. (e) Bright elongation. (f) Bright shortening.

where T_{spi} indicates the spiking threshold and α_7 is a scale parameter affecting the firing rate, that is, increasing it will bring about higher spiking frequency. Finally, the following formulation is used to indicate a potential collision threat in real-time robot experiments:

$$\text{Col}(t) = \begin{cases} \text{True}, & \text{if } \sum_{i=t-n_{ts}}^{t} S^{\text{spike}}(i) \geq n_{sp} \\ \text{False}, & \text{otherwise} \end{cases} \tag{28}$$

where n_{sp} denotes the number of spikes in a specified time window constituted by n_{ts} successive digital signal frames.

G. Setting Model Parameters

The parameters set up is described in Table I. The proposed visual neural network is featured by a feedforward structure. All the parameters are decided empirically with considerations and optimizations of the functionality of proposed biologically plausible pathways and mechanisms to implement a biological LGMD2 neuron, and moreover as an embedded vision system in a miniaturized mobile robot. There is currently no learning method involved for setting the parameters. However, these can be searched or learned in evolutionary computation, e.g., the genetic algorithms similar to the related bioinspired modeling studies [43], [58], since the search space of the proposed model is large and there are many parameters involved. As listed in Table I, the adaptable parameters, including C and R are decided by the physical property of input image sequences, that is, the resolution. More precisely, in the experiments, the video clips are 600×600 and 432×240

TABLE I
SETTING PARAMETERS OF THE PROPOSED LGMD2 MODEL

Parameter	Description	Value
n_p	luminance persistence in frames Eq. 1	$0 \sim 2$
α_1	coefficient in half-wave rectifying Eq. 3	0.1
τ_1	latency in ON channels Fig.2	$15 \sim 45$
τ_{in}	time interval of input digital signal	$30 \sim 50$
τ_2	latency in OFF channels Fig.2	$60 \sim 180$
w_3	bias baseline in ON channels	1
w_4	bias baseline in OFF channels	0.5
τ_3	latency in PM pathway Eq. 16	90
T_{pm}	threshold in PM pathway Eq. 17	10
$\{\theta_1, \theta_2, \theta_3\}$	term coefficients in S layer Eq. 18	$\{0.5, 1, 1\}$
C_ω	constant to calculate ω in Eq. 21	4
Δ_C	small real number in Eq. 22	0.01
C_{de}	decay coefficient in G layer	0.5
T_{de}	decay threshold in G layer	15
R, C	row, column of visual field in pixels	adaptable
α_5	coefficient in sigmoid function Eq. 24	$0.5 \sim 1$
τ_4	time constant in SFA Eq. 26	$500 \sim 1000$
T_{sfa}	small threshold in SFA	0.003
α_7	scale coefficient in spiking Eq. 27	4
T_{spi}	spiking threshold in Eq. 27	$0.65 \sim 0.78$
n_{ts}	time window by discrete digital frames	$4 \sim 8$
n_{sp}	number of spikes within n_{ts}	$6 \sim 8$

for synthetic and real-world input stimuli, respectively; the robot's field of view is set at 99×72.

The proposed LGMD2 model has been set up in Visual Studio (Microsoft Corporation). Data analysis and visualizations have been implemented in MATLAB (The MathWorks, Inc., Natick, MA, USA). Both the source code of algorithms and the neural-network layer outputs representing the signal processing in multiple layers or channels can be found at https://github.com/fuqinbing/LGMD2-open-source.

IV. EXPERIMENTAL RESULTS AND ANALYSIS

Within this section, systematic experiments are described which demonstrate how particular pathways and mechanisms contribute to the LGMD2's responses and selectivity. All the experiments can be categorized into two types of tests: 1) the offline tests and 2) the online tests. In the offline tests, the input stimuli consist of synthetic and recorded image streams. We compare the model responses and selectivity with the previous biological data on the LGMD2 [12] in Fig. 4. In the online tests, the proposed model is implemented in a miniaturized and vision-based mobile robot for real-time experiments.

A. Offline Tests

1) Synthetic Stimuli Testing: We start from testing the proposed model using computer-simulated movements. All the stimuli can be categorized into a few types, including approach, recession, translation, elongation, shortening, and sinusoidal grating following the physiological testing on the LGMD2.

First, we examine if the proposed model possesses similar unique selectivity like the biological LGMD2 as shown in Fig. 4. The results in Fig. 5 illustrate that the LGMD2 model responds selectively to darker looming object and is only shortly activated by recession of brighter object demonstrating the LGMD2's unique character. More precisely, when challenged against a darker approaching object, the LGMD2

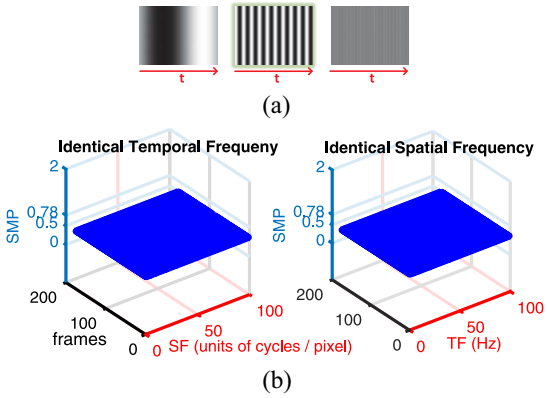

Fig. 8. LGMD2 outputs by sinusoidal gratings with a wide range of spatial frequency (SF) and temporal frequency (TF): the firing threshold is set at 0.78. (a) Varied grating stimuli. (b) Model outputs.

releases membrane potential that rapidly increases as the image size projected in the field of view grows. However, the LGMD2 model shows no response to the darker object that recedes. For a lighter (or white) looming object, the LGMD2 model remains quiet and is briefly activated during the start of recession. The proposed modeling of biased-ON and OFF pathways and SFA mechanism work effectively to achieve the required selectivity to darker objects with a preference for only OFF contrast.

Second for the stimuli restricted to the *X–Y* plane, with darker or brighter object translations at constant speed, the LGMD2 model only shows a brief, weak response at the beginning of each course (see Fig. 6), which conforms to the biological research [12] (Fig. 4). Importantly, the LGMD2 responds to translations regardless of motion directions, which is different to the neural systems with direction selectivity to the *X–Y* plane movements, e.g., [43], [52], and [56]. As a special case of translating stimuli, the elongation and shortening movements represent the situations that objects translate very close to the field of view (Fig. 7). More precisely, the single translating edge leads to OFF contrast during dark elongating and light shortening; otherwise, it gives rise to ON contrast. Similar to the physiological results in Fig. 4, the proposed LGMD2 model responds selectively and briefly to the dark elongating and light shortening stimuli with OFF contrast.

Finally, in the synthetic stimuli tests, we test the LGMD2 model using sinusoidal grating movements with a wide range of spatial and temporal frequencies, which is a basic test for examining the robustness of biologically inspired visual systems performing against various dynamic and cluttered backgrounds [17]. Fig. 8 demonstrates that the proposed LGMD2 model is not responding to the grating stimuli with varied spatiotemporal frequencies at all. The proposed original modeling of adaptive inhibition mechanism plays an important role to mediate lateral inhibitions suppressing the neuron against gratings. The results indicate that the proposed artificial neural network is robust to perform against a variety of dynamic and cluttered backgrounds.

2) Real Physical Stimuli Testing: After that, the proposed LGMD2 model is tested using recorded real-world visual stimuli, including indoor scenes and outdoor ground vehicle scenarios. Notably, compared with the simulated scenes, there

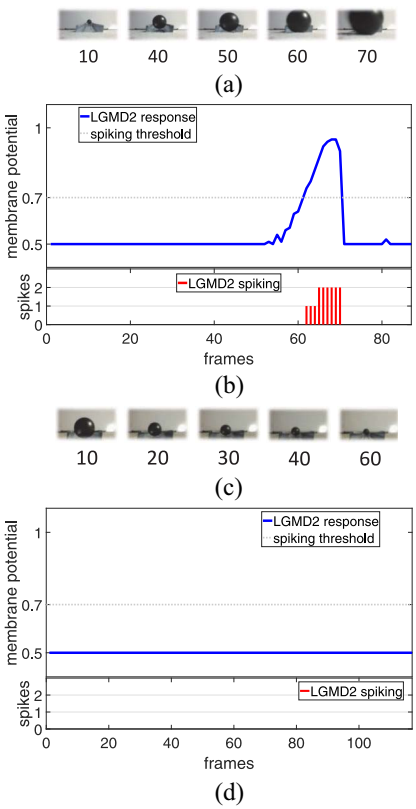

Fig. 9. LGMD2 outputs including potential and spike by a darker object approaching and receding within a bright background in a real physical scene. (a) Looming stimuli. (b) and (d) Model outputs. (c) Receding stimuli.

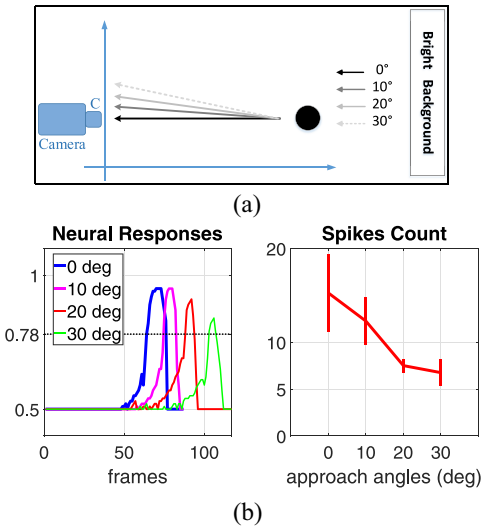

Fig. 10. Systematic angular-approach testing: (a) setting the experiments and (b) LGMD2 outputs by a darker object approaching with four distinct angles, and the statistical results of spikes elicited during every course each repeated ten times due to irregular approaching speed and light flash.

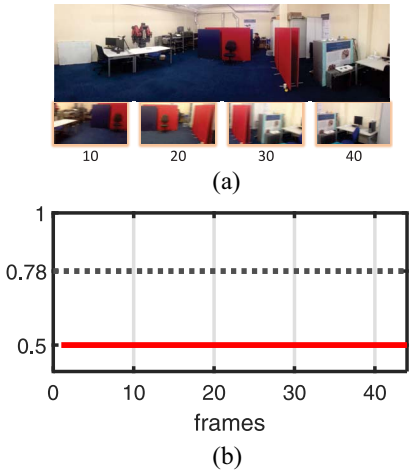

Fig. 11. LGMD2 model processes a rapid turning cluttered scene. (a) Wide-field stimuli. (b) Model output.

is much more background noise in the real physical world noise, such as light flash, shadows, etc. In addition, unlike the simulated movements, the object's moving speeds could not be maintained at a constant level. Therefore, the visual challenges presented to the model are "real."

First, in these tests, the LGMD2 model is tested by a darker object moving in depth within a bright background. As illustrated in Fig. 9, the LGMD2 responds selectively to darker object approaching instead of receding.

Second, we look deeper into the model performance against angular looming stimuli where the object (in Fig. 9) approaches on with an increased deviation from a direct collision trajectory, as illustrated in Fig. 10(a). The statistical results in Fig. 10(b) demonstrate the LGMD2 spikes at the highest frequency by direct looming stimuli. Along with the approach angle increasing, the LGMD2's output peaks later, and the peak response declines. Though other angular approaches could also activate the neuron, the spike frequency becomes much lower as the object moves away with a larger deviation. As introduced in Sections I and II, the locust looming detectors respond most strongly to objects that signal rapid and direct collision threat [15], [37]. The aforementioned OF-based methods and DSNs models can better recognize the angular approaches with different deviations from a direct collision trajectory, since the additional direction information can be extracted by those models. On the other hand, the LGMD2 model cannot tell the directions of translating edges as demonstrated by the translation testing results in Figs. 6 and 7 and the biological recordings in Fig. 4.

After that, we also test the proposed model using a rapid turning cluttered indoor scene with transient luminance change over the entire visual field. As shown in Fig. 11, the LGMD2 is rigorously inhibited during the whole-field movement. Similar to the grating tests in Fig. 8, the proposed adaptive inhibition mechanism works effectively to amplify the lateral inhibitions in the ON and OFF pathways to suppress the LGMD2 when dealing with such situations.

In the last type of offline experiments, we investigate the LGMD2's collision detection ability in much more complex and dynamic vehicle driving scenes using recordings from dashboard cameras as the input stimuli. Every scenario contains an urgent crash. Fig. 12 demonstrates the LGMD2 model can well perceive the impending crash representing high-spike frequency. Though some isolated spikes could be evoked by noncolliding motions, the LGMD2 spikes at a very high rate at the critical moments of threats detected. The

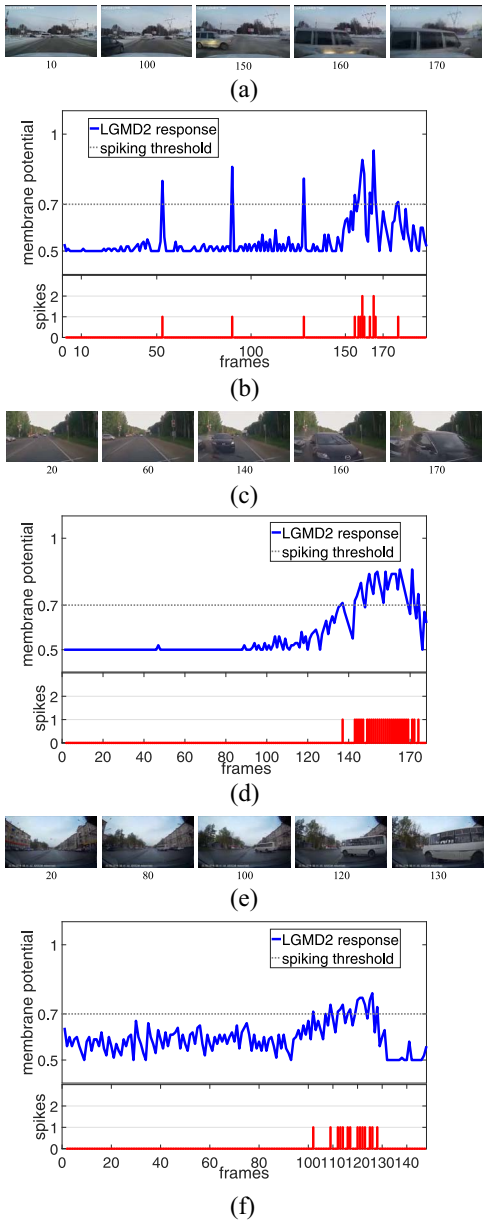

Fig. 12. LGMD2 model processes driving scenarios of ground vehicles. (a), (c), and (e) Crash video clips. (b), (d), and (f) LGMD2 outputs.

results show the great potential of the LGMD2 model to build collision-detecting visual systems for ground vehicles.

B. Online Robot Tests

Within this section, the online robot tests will be presented. The proposed LGMD2 has been successfully implemented as an embodiment in robot vision. The experiments can be categorized into two types of tests.

1) *Arena tests:* The robot agent is set at different constant linear speeds, and tested in an arena for collision perception and avoidance in near range navigation mixed with many obstacles.
2) *Bio-robotic tests:* The robot agent is tested by overhead approaching stimuli by different grayscale objects mimicking the situation that a juvenile locust on the ground is stimulated by strikes from predators in the bright sky.

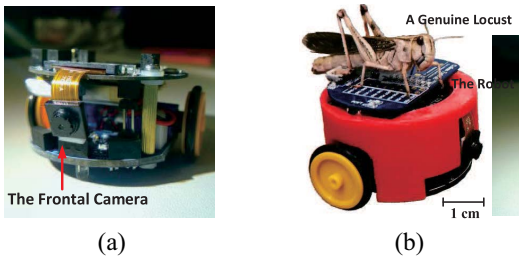

Fig. 13. Micro-mobile robot prototype: (a) *Colias* microrobot used in this article with a monocular camera as the only applied sensor for collision detection and (b) genuine locust on top of *Colias* demonstrating its small size.

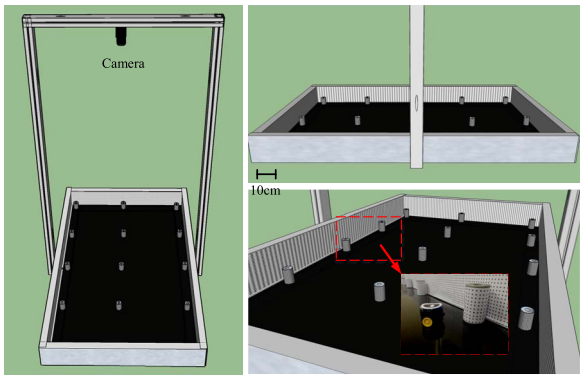

Fig. 14. Schematic illustration of the arena built on a TV screen with the size of 1430 (in length) $\times$805 (in width) $\times$150 (in height) mm^3. A CCD camera is set on the top of the arena to record the robot performance and run a real-time localization system [62]. There are poles as the obstacles in the arena. The walls and surfaces of the poles are decorated with densely distributed dark patterns to stimulate the mobile robot agent.

1) Robot Configuration: The mobile robot platform used in the online experiments is called *Colias*, as illustrated in Fig. 13. It is a vision-based ground micro robot developed for swarm robotic applications [59]–[61] and bio-robotics research [17], [24], [41]. The *Colias* robot has two primary boards. The bottom board actuates motion with a maximum speed of 35 cm/s. The upper board executes vision with an RGB miniaturized camera, as the only applied sensor in this article, which is capable of operating greater than 30 frames/s. The view angle could reach approximately 70°.

More specifically, for image processing, the *Colias* robot has limited computation resources. The microcontroller is an ARM Cortex-M4F core, which is deployed as the main processor for monitoring all the modules and serving the task. The 32-bit MCU STM32F427 clocked at 180 MHz provides the necessary computational power to have a real-time image stream processing. Its 256 KB internal SRAM supports the image buffering and computing.

2) Robot Arena Tests: In the first type of robot experiments, we examine the effectiveness and robustness of the proposed LGMD2 model for guiding the mobile robot for timely collision detection and avoidance in near range navigation in an arena, as depicted in Fig. 14. A *Colias* robot with the embedded LGMD2 module, as the only collision sensing modality, has been tested in the arena mixed with many obstacles.[1] There

[1]The videos are with https://github.com/fuqinbing/LGMD2-open-source.

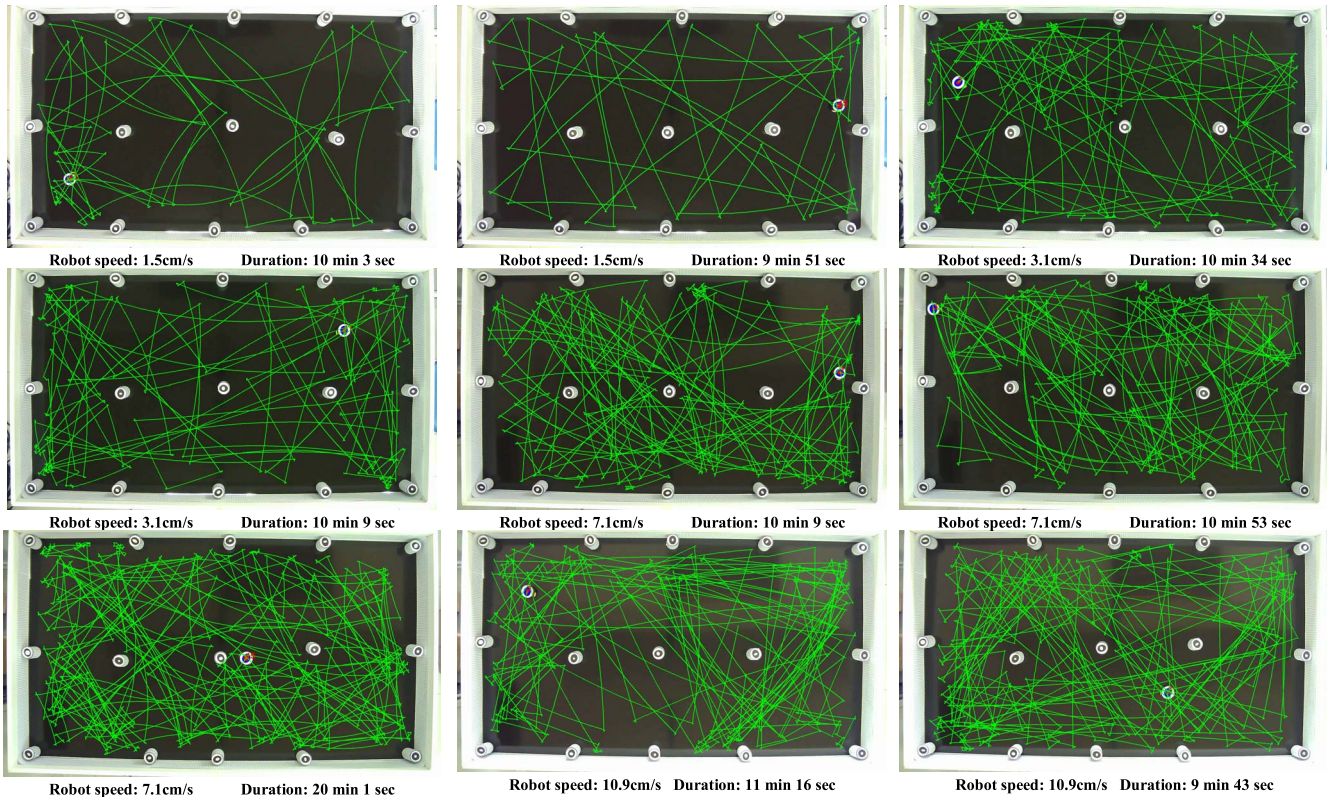

Fig. 15. Example results of the *Colias* robot arena tests for collision avoidance performance represented by trajectories over time (green line). The ID-specific agent has been tested with different constant linear velocities.

TABLE II
SRs OF COLLISION DETECTION IN ARENA TESTS

Speed(cm/s)	Avoidance	Miss-detection	Success rate(%)
0.1	69	101	40.59%
1.5	506	44	92.0%
3.5	1250	27	97.89%
7.1	1703	46	97.37%
10.9	1755	71	96.11%
15.4	1841	112	94.27%
17.1	1436	128	91.82%
27.3	196	21	90.32%
35.0	743	68	91.62%

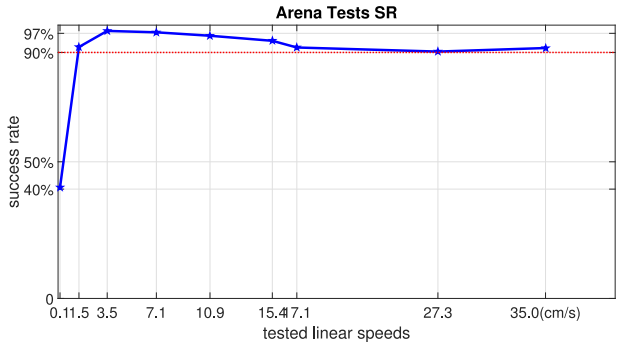

Fig. 16. SRs of the *Colias* agent through repeated arena tests at nine individual linear speeds for collision perception and avoidance.

are specific patterns on top of the agent and the obstacles for implementing a real-time localization system [62], in order to obtain the very precise trajectories of the ID-specific mobile robot and calculate the success rate (SR). In the arena tests, the goalless agent is initialized to go forward autonomously until a potential collision threat detected. The avoidance behavior is simply set to turn right or left randomly with a large angle, as the mobile robot can only run on the 2-D surface. After each avoidance, the agent resumes its forward motion, and so on. Moreover, the constant linear speed of tested agent is set at nine levels ranging from extremely slow (0.1 cm/s) to the maximum speed (35 cm/s).

Fig. 15 illustrates some arena test results with robot over-time trajectories. In general, the robot agent performs consistently and robustly for timely collision perception and avoidance in the arena interacting with obstacles and periphery walls. However, we have noticed the wall issues, with which if the robot gets too close to the wall after turning, it may fail in detecting the collision. In addition, the visual coverage is also limited, with which the robot cannot "see" the poles in some cases. Table II and Fig. 16 demonstrate statistical SRs at different tested velocities throughout repeated tests, which can be denoted by

$$\mathrm{SR} = \mathrm{EV}_a/(\mathrm{EV}_a + \mathrm{EV}_m) \tag{29}$$

where EV_a and EV_m indicate the specified events of collision avoidance and miss-detection (hitting the poles or surrounding walls with human intervention during experiments).

The arena test results have verified the flexibility and robustness of the proposed LGMD2 model on the embedded system

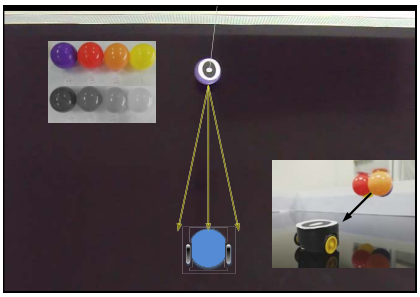

Fig. 17. Setting the bio-robotic looming tests in the arena using objects at four different gray levels as the stimuli. Every grayscale overhead looming course is repeated a hundred times due to irregular approaching speed and angle and light flash. The yellow arrows indicate the scope of looming directions, including direct and angular approaches.

to guide mobile machines for collision detection in navigation. More concretely, except for the extremely slow speed of 0.1 cm/s, the SRs are all above 90% with satisfactory performance.

3) Bio-Robotic Looming Tests: A physiological research has recently revealed that the LGMD2 neuron plays a crucial role in juvenile locusts that mainly live on the ground to recognize the proximity of darker targets, e.g., strike from predators in the bright sky [14]. As the first systematic model system to carry out the LGMD2's specific functions, we have also designed bio-robotic tests mimicking the similar scenarios for deepening our understanding of the LGMD2's unique characteristics.

A *Colias* agent with the LGMD2 visual system is set up in the arena and stimulated by four overhead approaching objects, respectively, each with certain grayscale. The experimental setting is illustrated in Fig. 17. Notably, all objects are darker than their background (the wall of the arena): the violet one is the darkest object whilst the yellow one has the smallest contrast to its background. In this kind of experiment, the robot collision avoidance behavior is configured the same to the arena tests. There are also specific patterns on the top of approaching objects for localization. Therefore, we can track the moving objects, and then obtain the exact positions indicating the activation of robot collision avoidance behavior.

The following analyses can be drawn from Fig. 18.

1) The LGMD2 agent is able to detect every grayscale darker object that approaches overhead corresponding to a timely evasive move.
2) The LGMD2 model is more sensitive to looming stimuli caused by objects with larger contrast to the background. More precisely, the darker looming objects lead to more frequent avoidance behaviors with relatively longer reaction distances to collision threats; on the other hand, the looming object with the smallest contrast rarely activate the LGMD2 agent with relatively shortest reaction distances to collision threats.
3) The LGMD2 agent responds more constantly to darker objects that approach directly than other angular approaches. The results reconcile with the revealed properties of locust's LGMDs, which respond most strongly to objects signaling frontal collision threats [15], [17], [37]. This also well matches the angular approach test results in Fig. 10.

To summarize, the online tests results have demonstrated our achievements on two main aspects.

1) The proposed LGMD2 model has robust performance in the micro-mobile robot for collision detection that could be built as low cost, energy efficient, and miniaturized visual sensors for mobile machines.
2) The locust LGMD2's specific selectivity to darker objects has been achieved by the proposed computational modeling.

V. Further Discussion

Through the above systematic experiments, we have shown that the proposed LGMD2 visual neural network, with parallel biased-ON and OFF pathways and adaptive lateral inhibitions, demonstrates the similar characteristics and selectivity to biological LGMD2 neurons in the locust's visual systems. In locusts, both the LGMD1 and the LGMD2 respond to a rapid expanding image of an approaching object representing an imminent collision or a strike from predator [11], [12], [15]. Nevertheless, the biological functions of LGMD2 differ from the LGMD1 in a number of ways [12]. First, the LGMD2 is not sensitive to a brighter or white looming object whereas the LGMD1 is. Second, the LGMD2 does not respond to darker objects that recede at all, while the LGMD1 is often excited though very briefly. The proposed computational model has fully exhibited the above two critical features, as shown in Figs. 5 and 9. The model's selectivity to only OFF contrast also satisfies with the biological data in Fig. 4.

The LGMD2 matures earlier than the LGMD1 and plays a crucial role of sensing predators for juvenile locusts living on the ground [14]. As the locusts grow up, the visual environments become more complex due to flying behaviors [63], [64]. The LGMD1 gradually complements the LGMD2 and can deal with other flight-related colliding scenarios. A possible reason is that the LGMD1 can recognize also brighter looming objects. However, the LGMD2 still exists in the visual pathways of adult locusts. How both neurons cooperate in the locust's looming perception neural system is still unknown. From a modeler's perspective, a possible way is to build multiple visual pathways combining both the LGMDs to investigate the looming perception in different environments.

It is worth emphasizing that the "darker object" in this article is relative to the brightness of its background. As shown in the experiments, e.g., Fig. 12, a white vehicle is still darker than the bright sky as the background, so the imminent crash is detected; while it is hard to find a brighter object approaching against dark background in real world (see experiments in Fig. S3 of the supplementary material).

There are different methods for shaping the selectivity in such looming sensitive models or neural networks. For example, Badia *et al.* [18] proposed that the high nonlinearity between the feedforward excitatory and inhibitory responses can well form the selectivity to approaching objects. The FFI pathway in the LGMD1 model, e.g., [11], [41], and [51] can

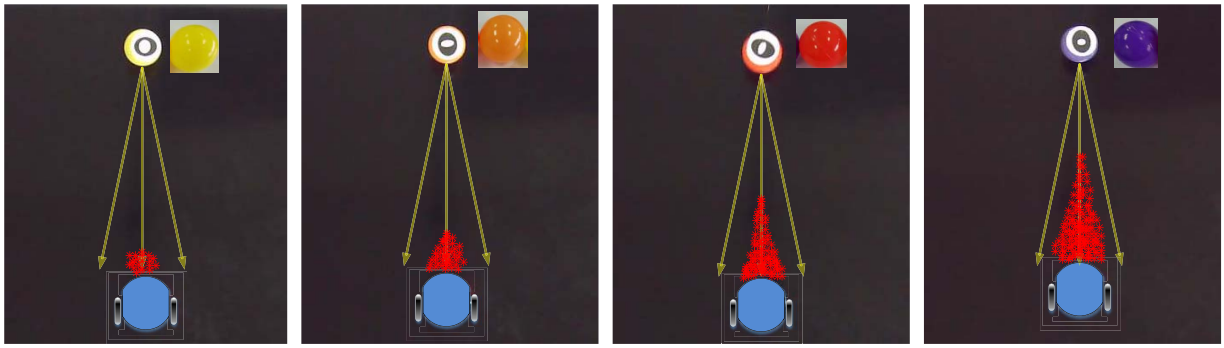

Fig. 18. Illustrations of the locations marked by red asterisks where the avoidance behavior of the tested robot agent is aroused by overhead looming objects throughout repeated tests under the setting in Fig. 17. The markings of some positions are overlapped.

also adjust the selectivity at some critical moments, such as the end of approach and the start of recession, which cannot be disregarded. In this article, the proposed adaptive inhibition mechanism in the LGMD2 is also an effective approach to make the neuron adaptive to different background motion complexity. Combined with a recent LGMD1 modeling study [17], the bio-plausible structure of ON and OFF pathways could play a role in the locust's visual system to separate the distinct selectivity between the LGMD1 and the LGMD2. In addition, recent research demonstrates a self-inhibition mechanism could coordinate with the lateral inhibition to further sharpen up the LGMDs' selectivity to looming versus translation stimuli [15]. In the future, we will investigate these different mechanisms with challenges from a variety of real-world applications.

VI. Conclusion

This article has presented a collision perception visual neural network based on a unique neuron LGMD2 in the locust's visual pathway. The LGMD2 is sensitive to looming objects but only responds selectively to darker objects that approach against bright background underlying a preference for OFF contrast. We have proposed the original computational modeling of biased-ON and OFF pathways with an adaptive inhibition mechanism to fulfill the LGMD2's specific selectivity and characteristics for the perception of darker looming objects. The proposed approach has been validated with systematic experiments ranging from synthetic stimuli tests to real world, including vehicle driving scenarios and online robot tests. The experimental results have demonstrated the robustness and flexibility of the proposed LGMD2 visual neural network for collision perception against various dynamic and cluttered backgrounds. The LGMD2 model can be a good candidate visual system to build low-cost and energy-efficient collision-detecting sensors for mobile robots and autonomous vehicles. Similar to other neuromorphic computation structures, the proposed method can be easily realized in a very large scale integration (VLSI) chip for volume production.

References

[1] J. Thorson, "Small-signal analysis of a visual reflex in the locust. I. Input parameters," *Kybernetik*, vol. 3, no. 2, pp. 41–53, 1966.

[2] J. S. Kennedy, "The migration of the desert locust (schistocerca gregaria forsk.) I. The behaviour of swarms. II. A theory of long-range migrations," *Philos. Trans. Roy. Soc. London B Biol. Sci.*, vol. 235, pp. 163–290, May 1951.

[3] E. Warrant and M. Dacke, "Visual navigation in nocturnal insects," *Physiology*, vol. 31, no. 3, pp. 182–192, 2016.

[4] E. Baird, E. Kreiss, W. Wcislo, E. Warrant, and M. Dacke, "Nocturnal insects use optic flow for flight control," *Biol. Lett.*, vol. 7, no. 4, pp. 499–501, 2011.

[5] J. R. Serres and F. Ruffier, "Optic flow-based collision-free strategies: From insects to robots," *Arthropod Struct. Develop.*, vol. 46, no. 5, pp. 703–717, 2017.

[6] Q. Fu, C. Hu, P. Liu, and S. Yue, "Towards computational models of insect motion detectors for robot vision," in *Proc. Towards Auton. Robot. Syst. Conf.*, 2018, pp. 465–467.

[7] N. Franceschini, "Small brains, smart machines: From fly vision to robot vision and back again," *Proc. IEEE*, vol. 102, no. 5, pp. 751–781, May 2014.

[8] Q. Fu, H. Wang, C. Hu, and S. Yue, "Towards computational models and applications of insect visual systems for motion perception: A review," *Artif. Life*, vol. 25, no. 3, pp. 263–311, 2019.

[9] M. O'Shea and J. L. D. Williams, "The anatomy and output connections of a locust visual interneurone: The lobular giant movement detector (LGMD) neurone," *J. Comput. Physiol.*, vol. 91, no. 3, pp. 257–266, 1974.

[10] M. O'Shea and C. H. F. Rowell, "The neuronal basis of a sensory analyser, the acridid movement detector system. II. Response decrement, convergence, and the nature of the excitatory afferents to the fan-like dendrites of the LGMD," *J. Exp. Biol.*, vol. 65, no. 2, pp. 289–308, 1976.

[11] F. C. Rind and D. I. Bramwell, "Neural network based on the input organization of an identified neurone signaling impending collision," *J. Neurophysiol.*, vol. 75, no. 3, pp. 967–985, 1996.

[12] P. J. Simmons and F. C. Rind, "Responses to object approach by a wide field visual neurone, the LGMD2 of the locust: Characterization and image cues," *J. Comparative Physiol. Sensory Neural Behav. Physiol.*, vol. 180, no. 3, pp. 203–214, 1997.

[13] S. Wernitznig *et al.*, "Synaptic connections of first-stage visual neurons in the locust schistocerca gregaria extend evolution of tetrad synapses back 200 million years," *J. Comput. Neurol.*, vol. 523, no. 2, pp. 298–312, 2015.

[14] J. Sztarker and F. C. Rind, "A look into the cockpit of the developing locust: Looming detectors and predator avoidance," *Develop. Neurobiol.*, vol. 74, no. 11, pp. 1078–1095, 2014.

[15] F. C. Rind *et al.*, "Two identified looming detectors in the locust: Ubiquitous lateral connections among their inputs contribute to selective responses to looming objects," *Sci. Rep.*, vol. 6, Oct. 2016, Art. no. 35525.

[16] S. Yue and F. C. Rind, "A collision detection system for a mobile robot inspired by locust visual system," in *Proc. IEEE Int. Conf. Robot. Autom.*, 2005, pp. 3843–3848.

[17] Q. Fu, C. Hu, J. Peng, and S. Yue, "Shaping the collision selectivity in a looming sensitive neuron model with parallel ON and OFF pathways and spike frequency adaptation," *Neural Netw.*, vol. 106, pp. 127–143, Oct. 2018.

[18] S. B. I. Badia, U. Bernardet, and P. F. Verschure, "Non-linear neuronal responses as an emergent property of afferent networks: A case study of the locust lobular giant movement detector," *PLoS Comput Biol.*, vol. 6, no. 3, 2010, Art. no. e1000701.

[19] P. Cizek, P. Milicka, and J. Faigl, "Neural based obstacle avoidance with CPG controlled hexapod walking robot," in *Proc. IEEE Int. Joint Conf. Neural Netw. (IJCNN)*, 2017, pp. 650–656.

[20] L. Salt, G. Indiveri, and Y. Sandamirskaya, "Obstacle avoidance with LGMD neuron: Towards a neuromorphic UAV implementation," in *Proc. IEEE Int. Symp. Circuits Syst. (ISCAS)*, 2017, pp. 1–4.

[21] J. Zhao, X. Ma, Q. Fu, C. Hu, and S. Yue, "An LGMD based competitive collision avoidance strategy for UAV," in *Artificial Intelligence Applications and Innovations. AIAI 2019* (IFIP Advances in Information and Communication Technology), vol. 559, J. MacIntyre, I. Maglogiannis, L. Iliadis, and E. Pimenidis, Eds. Cham, Switzerland: Springer, 2019, pp. 80–91.

[22] A. Borst and T. Euler, "Seeing things in motion: Models, circuits, and mechanisms," *Neuron*, vol. 71, no. 6, pp. 974–994, 2011.

[23] A. Borst and M. Helmstaedter, "Common circuit design in fly and mammalian motion vision," *Nat. Neurosci.*, vol. 18, no. 8, pp. 1067–1076, 2015.

[24] Q. Fu, S. Yue, and C. Hu, "Bio-inspired collision detector with enhanced selectivity for ground robotic vision system," in *Proc. Brit. Mach. Vis. Conf.*, 2016, pp. 1–13.

[25] Q. Fu, C. Hu, T. Liu, and S. Yue, "Collision selective LGMDs neuron models research benefits from a vision-based autonomous micro robot," in *Proc. IEEE Int. Conf. Intell. Robots Syst.*, 2017, pp. 3996–4002.

[26] Q. Fu and S. Yue, "Modelling LGMD2 visual neuron system," in *Proc. IEEE 25th Int. Workshop Mach. Learn. Signal Process.*, 2015, pp. 1–6.

[27] A. Mukhtar, L. Xia, and T. B. Tang, "Vehicle detection techniques for collision avoidance systems: A review," *IEEE Trans. Intell. Transp. Syst.*, vol. 16, no. 5, pp. 2318–2338, Oct. 2015.

[28] G. N. DeSouza and A. C. Kak, "Vision for mobile robot navigation: A survey," *IEEE Trans. Pattern Anal. Mach. Intell.*, vol. 24, no. 2, pp. 237–267, Feb. 2002.

[29] F. Poiesi and A. Cavallaro, "Detection of fast incoming objects with a moving camera," in *Proc. Brit. Mach. Vis. Conf.*, 2016, pp. 1–11.

[30] D. Holz, S. Holzer, R. B. Rusu, and S. Behnke, "Real-time plane segmentation using RGB-D cameras," in *Proc. RoboCup Robot Soccer World Cup XV*, 2012, pp. 306–317.

[31] B. Peasley and S. Birchfield, "Real-time obstacle detection and avoidance in the presence of specular surfaces using an active 3D sensor," in *Proc. IEEE Workshop Robot Vis.*, 2013, pp. 197–202.

[32] H. Kim, S. Leutenegger, and A. J. Davison, "Real-time 3D reconstruction and 6-DoF tracking with an event camera," in *Proc. Eur. Conf. Comput. Vis.*, 2016, pp. 349–364.

[33] A. R. Vidal, H. Rebecq, T. Horstschaefer, and D. Scaramuzza, "Ultimate SLAM? Combining events, images, and IMU for robust visual SLAM in HDR and high speed scenarios," *IEEE Robot. Autom. Lett.*, vol. 3, no. 2, pp. 994–1001, Apr. 2018.

[34] W. E. Green and P. Y. Oh, "Optic-flow-based collision avoidance," *IEEE Robot. Autom. Mag.*, vol. 15, no. 1, pp. 96–103, Mar. 2008.

[35] J. Serres and F. Ruffier, "Optic flow-based robotics," in *Wiley Encyclopedia of Electrical and Electronics Engineering*, Amer. Cancer Soc., 2016, pp. 1–14. [Online]. Available: https://onlinelibrary.wiley.com/doi/abs/10.1002/047134608X.W8321, doi: 10.1002/047134608X.W8321.

[36] F. C. Rind and P. J. Simmons, "Seeing what is coming: Building collision sensitive neurons," *Trends Neurosci.*, vol. 22, no. 5, pp. 215–220, 1999.

[37] J. M. Yakubowski, G. A. Mcmillan, and J. R. Gray, "Background visual motion affects responses of an insect motion-sensitive neuron to objects deviating from a collision course," *Physiol. Rep.*, vol. 4, no. 10, 2016, Art. no. e12801.

[38] S. Yue, F. C. Rind, M. S. Keil, J. Cuadri, and R. Stafford, "A bio-inspired visual collision detection mechanism for cars: Optimisation of a model of a locust neuron to a novel environment," *Neurocomputing*, vol. 69, nos. 13–15, pp. 1591–1598, 2006.

[39] M. Hartbauer, "Simplified bionic solutions: A simple bio-inspired vehicle collision detection system," *Bioinspiration Biomimetics*, vol. 12, no. 2, 2017, Art. no. 026007.

[40] Q. Fu, N. Bellotto, H. Wang, F. C. Rind, H. Wang, and S. Yue, "A visual neural network for robust collision perception in vehicle driving scenarios," in *Artificial Intelligence Applications and Innovations. AIAI 2019* (IFIP Advances in Information and Communication Technology), vol. 559, J. MacIntyre, I. Maglogiannis, L. Iliadis, and E. Pimenidis, Eds. Cham, Switzerland: Springer, 2019, pp. 67–79.

[41] C. Hu, F. Arvin, C. Xiong, and S. Yue, "Bio-inspired embedded vision system for autonomous micro-robots: The LGMD case," *IEEE Trans. Cogn. Develop. Syst.*, vol. 9, no. 3, pp. 241–254, Sep. 2017.

[42] H. Meng *et al.*, "A modified model for the lobular giant movement detector and its FPGA implementation," *Comput. Vis. Image Understanding*, vol. 114, no. 11, pp. 1238–1247, 2010.

[43] S. Yue and F. C. Rind, "Postsynaptic organization of directional selective visual neural networks for collision detection," *Neurocomputing*, vol. 103, pp. 50–62, Mar. 2013.

[44] A. Riehle and N. Franceschini, "Motion detection in flies: Parametric control over ON-OFF pathways," *Exp. Brain Res.*, vol. 54, no. 2, pp. 390–394, 1984.

[45] J. Antolik, "Rapid long-range disynaptic inhibition explains the formation of cortical orientation maps," *Front. Neural Circuits*, vol. 11, no. 21, 2017, Art. no. 00021.

[46] T. W. Troyer, A. E. Krukowski, N. J. Priebe, and K. D. Miller, "Contrast-invariant orientation tuning in cat visual cortex: Thalamocortical input tuning and correlation-based intracortical connectivity," *J. Neurosci.*, vol. 18, no. 15, pp. 5908–5927, 1998.

[47] L. Chariker, R. Shapley, and L.-S. Young, "Orientation selectivity from very sparse LGN inputs in a comprehensive model of macaque V1 cortex," *J. Neurosci.*, vol. 36, no. 49, pp. 12368–12384, 2016.

[48] S. D. Wiederman, P. A. Shoemaker, and D. C. O'Carroll, "Correlation between off and on channels underlies dark target selectivity in an insect visual system," *J. Neurosci.*, vol. 33, no. 32, pp. 13225–13232, 2013.

[49] A. C. James and D. Osorio, "Characterisation of columnar neurons and visual signal processing in the medulla of the locust optic lobe by system identification techniques," *J. Comparative Physiol. A*, vol. 178, no. 2, pp. 183–199, 1996.

[50] M. S. Keil, E. Roca-Moreno, and A. Rodriguez-Vazquez, "A neural model of the locust visual system for detection of object approaches with real-world scenes," in *Proc. 4th IASTED Int. Conf. Visual. Imag. Image Process. (IASTED)*, 2004, pp. 340–345.

[51] S. Yue and F. C. Rind, "Collision detection in complex dynamic scenes using a LGMD based visual neural network with feature enhancement," *IEEE Trans. Neural Netw.*, vol. 17, no. 3, pp. 705–716, May 2006.

[52] H. Wang, J. Peng, and S. Yue, "A directionally selective small target motion detecting visual neural network in cluttered backgrounds," *IEEE Trans. Cybern.*, to be published.

[53] H. Wang, J. Peng, Q. Fu, H. Wang, and S. Yue, "Visual cue integration for small target motion detection in natural cluttered backgrounds," in *Proc. IEEE Int. Joint Conf. Neural Netw.*, 2019, pp. 1–7.

[54] H. Wang *et al.*, "Angular velocity estimation of image motion mimicking the honeybee tunnel centring behaviour," in *Proc. IEEE Int. Joint Conf. Neural Netw.*, 2019, pp. 1–7.

[55] H. Wang, Q. Fu, H. Wang, J. Peng, and S. Yue, "Constant angular velocity regulation for visually guided terrain following," in *Artificial Intelligence Applications and Innovations. AIAI 2019* (IFIP Advances in Information and Communication Technology), vol. 559, J. MacIntyre, I. Maglogiannis, L. Iliadis, and E. Pimenidis, Eds. Cham, Switzerland: Springer, 2019, pp. 597–608.

[56] Q. Fu and S. Yue, "Modeling direction selective visual neural network with on and off pathways for extracting motion cues from cluttered background," in *Proc. Int. Joint Conf. Neural Netw.*, 2017, pp. 831–838.

[57] Q. Fu, N. Bellotto, C. Hu, and S. Yue, "Performance of a visual fixation model in an autonomous micro robot inspired by drosophila physiology," in *Proc. IEEE Int. Conf. Robot. Biomimetics*, 2018, pp. 1802–1808.

[58] S. Yue and F. C. Rind, "Redundant neural vision systems—Competing for collision recognition roles," *IEEE Trans. Auton. Mental Develop.*, vol. 5, no. 2, pp. 173–186, Jun. 2013.

[59] C. Hu, Q. Fu, T. Liu, and S. Yue, "A hybrid visual-model based robot control strategy for micro ground robots," in *Proc. Animals Animats*, 2018, pp. 162–174.

[60] C. Hu, Q. Fu, and S. Yue, "Colias IV: The affordable micro robot platform with bio-inspired vision," in *Proc. Towards Auton. Robot. Syst. Conf.*, 2018, pp. 197–208.

[61] X. Sun, T. Liu, C. Hu, Q. Fu, and S. Yue, "ColCOS ϕ: A multiple pheromone communication system for swarm robotics and social insects research," in *Proc. IEEE 4th Int. Conf. Adv. Robot. Mechatron. (ICARM)*, 2019, pp. 59–66.

[62] T. Krajník *et al.*, "A practical multirobot localization system," *J. Intell. Robot. Syst.*, vol. 76, nos. 3–4, pp. 539–562, 2014.

[63] P. J. Simmons, J. Sztarker, and F. C. Rind, "Looming detection by identified visual interneurons during larval development of the locust locustar migratoria," *J. Exp. Biol.*, vol. 216, no. 12, pp. 2266–2275, 2013.

[64] P. J. Simmons, F. C. Rind, and R. D. Santer, "Escapes with and without preparation: The neuroethology of visual startle in locusts," *J. Insect. Physiol.*, vol. 56, no. 8, pp. 876–883, 2010.

Qinbing Fu (M'18) received the B.Sc. degree from the University of Electronic Science and Technology of China, Chengdu, China, in 2009, and the M.Sc. and Ph.D. degrees from the University of Lincoln, Lincoln, U.K., in 2014 and 2018, respectively.

He was a Research Assistant at the School of Mathematics and Statistics, Xi'an Jiaotong University, Xi'an, China, and the Institute of Microelectronics, Tsinghua University, Beijing, China, from 2014 to 2018. He is currently an Honorary Postdoctoral Research Fellow with the University of Lincoln, Lincoln, U.K., and a Postdoctoral Research Fellow with Guangzhou University, Guangzhou, China. His current research interests include computer vision, bio-inspired algorithms, bio-robotics, and machine learning.

Dr. Fu was a recipient of the Marie Curie Fellowship, involved in the EU FP7 Projects EYE2E (269118) and LIVCODE (295151), and EU Horizon 2020 Projects STEP2DYNA (691154) and ULTRACEPT (778062). He is a member of the Robotics and Automation Society and the International Neural Network Society.

Cheng Hu received the B.Eng. degree from the College of Opt-Electronics Engineering, Chongqing University, Chongqing, China, in 2013, and the Ph.D. degree from the University of Lincoln, Lincoln, U.K., in 2018.

He is currently an Honorary Postdoctoral Research Fellow with the University of Lincoln and a Postdoctoral Research Fellow with Guangzhou University, Guangzhou, China. His current research interests include bio-inspired algorithms, bio-robotics, autonomous robots, sensors, and signal processing.

Dr. Hu was a recipient of the Marie Curie Fellowship, involved in the EU FP7 Projects EYE2E (269118) and LIVCODE (295151), and EU Horizon 2020 Projects STEP2DYNA (691154) and ULTRACEPT (778062).

Jigen Peng received the B.Sc. degree from Jiangxi University, Nanchang, China, in 1989, and the M.Sc. and Ph.D. degrees from Xi'an Jiaotong University, Xi'an, China, in 1992 and 1998, respectively.

He is currently a Professor with the School of Mathematics and Information Science, Guangzhou University, Guangzhou, China. He was at Xi'an Jiaotong University, Xi'an, and the City University of Hong Kong, Hong Kong, until 2017. His current research interests include nonlinear functional analysis and applications, machine-learning theory, and sparse information processing.

F. Claire Rind received the B.Sc. degree in animal physiology from the University of Canterbury, Christchurch, New Zealand, in 1976, and the Ph.D. degree in zoology from Cambridge University, Cambridge, U.K., in 1982.

She is currently a Reader of invertebrate neuroscience with the School of Biology and with the Institute of Neuroscience, Newcastle University, Newcastle, U.K. Her current research interests include sensory processing by the insect brain, neuronal pathways for collision avoidance in locusts, bio-inspired robotics, and application-specific integrated circuits for visual tasks.

Dr. Rind was a recipient of the Royal Society University Research Fellowship, and the Biotechnology and Biological Sciences Research Council Advanced Research Fellowship. She is a member of the Society for Experimental Biology, the Physiological Society, and the International Society for Neuroethology.

Shigang Yue (M'05–SM'17) received the B.Eng degree from Qingdao Technological University, Qingdao, China, in 1988, and the M.Sc. and Ph.D. degrees from the Beijing University of Technology (BJUT), Beijing, China, in 1993 and 1996, respectively.

He was at BJUT as a Lecturer from 1996 to 1998 and as an Associate Professor from 1998 to 1999. He was an Alexander von Humboldt Research Fellow at the University of Kaiserslautern, Kaiserslautern, Germany, from 2000 to 2001. He held research positions at the University of Cambridge, Cambridge, U.K.; Newcastle University, Newcastle upon Tyne, U.K.; and University College London, London, U.K., from 2002 to 2007. In 2007, he joined the University of Lincoln, Lincoln, U.K., as a Senior Lecturer and was promoted to a Professor in 2012, where he is currently a Professor (part-time) with the School of Computer Science. He also holds a Professorship with the Machine Life and Intelligence Research Centre, Guangzhou University, Guangzhou, China, in collaboration with Prof. J. Peng. His current research interests include artificial intelligence, computer vision, robotics, intelligent transportation, brains, and neuroscience.

Prof. Yue is a member of the International Neural Network Society and the International Society of Bionic Engineering.